Inorganica Chimica Acta 486 (2019) 294–303

Contents lists available at ScienceDirect

Inorganica Chimica Acta

journal homepage: www.elsevier.com/locate/ica

Research paper

Synthesis, structures and antimicrobial activity of novel NHC*- and Ph_3P-Ag(I)-Benzoate derivatives

Cillian O'Beirne[a], Nada F. Alhamad[a], Qinxi Ma[b], Helge Müller-Bunz[a], Kevin Kavanagh[c], Geraldine Butler[b], Xiangming Zhu[a], Matthias Tacke[a,*]

[a] School of Chemistry, University College Dublin, Belfield, Dublin 4, Ireland
[b] UCD School of Biomolecular and Biomedical Science, Conway Institute, University College Dublin, Belfield, Dublin 4, Ireland
[c] Department of Biology, NUI Maynooth, Ireland

ARTICLE INFO

Keywords:
N-Heterocyclic carbenes
NHC-silver(I) complex
MRSA
Candida
Crystal structures
Antimicrobial resistance

ABSTRACT

The rising threat of Antimicrobial Resistance (AMR) requires a novel approach to the treatment of infectious diseases. Covalently bonded silver, which has known antibacterial and antifungal properties and multiple mechanisms of action, may provide a treatment strategy when used alone or in combination with already known antimicrobial compounds. Here we describe the synthesis of eight novel silver(I) complexes, which were screened for *in vitro* activity against two pathogenic bacterial strains, *Methicillin-resistant Staphylococcus aureus* (*MRSA*) and *Escherichia coli* (*E. coli*), and against two pathogenic fungal strains, *Candida albicans* and *Candida parapsilosis*. Complexes **5–8** were synthesized by reacting triphenylphosphine in relative equivalents with the relevant silver benzoates (**1**, **2** & **4**), whilst complexes **9–12** were synthesized by generation of a free carbene NHC* (1,3-dibenzyl-4,5-diphenyl-imidazol-2-ylidene) and reacting this with the silver benzoates **1–4**, under Schlenk conditions. Complexes **9–12** showed the strongest antimicrobial activity, resulting in 50% inhibition of growth against *MRSA* and *C. parapsilosis* at concentrations of 12.5 and 3.25 μg/mL, respectively.

1. Introduction

In the fight against Antimicrobial Resistance (AMR) there is increased interest in the use of silver based antimicrobials as a route to developing new classes of drugs to overcome resistance [1,2]. Silver has a long history in clinical medicine as a key component in burn wound creams [3] and it has recently been shown to enhance the activity of frontline antibiotics [4].There are few reports of prolonged resistance [5] with only recent, isolated examples occurring after decades of use [6].

In the last five years the growth of AMR across the world has been highlighted in reports by the Centre for Disease Control (CDC) [7], World Health Organisation (WHO) [8] and the European Centre for Disease Prevention and Control (ECDC) [9]. The increasing risk of further resistance is in part due to the over-use of antimicrobials [10] and also the failure to develop new drugs with multiple mechanisms of action to replace or supplement already undermined antimicrobial compound classes [10,11]. Using the requirement of multiple mechanisms of action as an objective for future antimicrobial development, silver presents an interesting element for use as a central antimicrobial moiety. Silver sulfadiazine has been used since the early 1960s to consistently treat burn wounds [12] and it has been shown that the bioavailability of Ag^+ cations in antimicrobials is essential for its multiple effects on microbial cells [13]. Although the mechanisms of action have yet to be fully elucidated, in bacterial cells silver has been shown to cause cell wall damage [14,15], intracellular protein disruption [14], stress induced seizure of DNA [14,15], disruption of bacterial cell proton motive force [16], ATP synthesis disruption [17] and an increase in Reactive Oxygen Species (ROS) due to iron-sulphur cluster disruption [18].

Suitable biomolecules can be incorporated in order to enhance the bioavailability of silver and also to act as supplementary antimicrobial agents [19,20]. For this purpose the use of *N*-heterocyclic carbenes (NHCs) and phosphines can be used to form suitably bioavailable complexes for use as antimicrobial agents [20,21]. Previous work by our group has highlighted the use of the lipophilic NHC* (1,3-dibenzyl-4,5-diphenyl imidazol-2-ylidene) ligand to produce effective silver complexes with antimicrobial activity against several strains of pathogenic bacteria, including *Methicillin-resistant Staphylococcus aureus* (*MRSA*) [22,23]. Along with this promising activity, the lead compound in this class of NHC-silver(I) acetate complexes, SBC3 (Fig. 1), has shown good activity against *Candida albicans* in an invertebrate *in vivo*

* Corresponding author.
E-mail address: matthias.tacke@ucd.ie (M. Tacke).

https://doi.org/10.1016/j.ica.2018.10.057
Received 25 September 2018; Received in revised form 25 October 2018; Accepted 26 October 2018
Available online 27 October 2018
0020-1693/

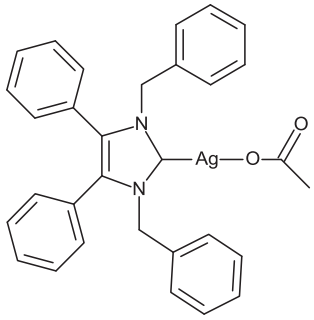

Fig. 1. Structure of the antibiotic lead compound SBC3 [22].

model, demonstrating broad spectrum activity against both bacteria and fungi [24], and demonstrating it is well tolerated *in vivo*. Optimisation and testing of these first generation complexes [22,25] has led to the development of eight novel silver complexes, four triphenylphosphino-silver(I) benzoate complexes (**5–8**) and four NHC*-silver(I) benzoate complexes (**9–12**). Previously it was shown that the imidazolium salt of our complexes produces a minor antibiotic effect [22] and so with the incorporation of benzoates in tandem with this NHC*-moiety it is hoped that a more pronounced antimicrobial effect will occur.

In this work we present the synthesis and biological evaluation of eight new silver(I) complexes and their antimicrobial activity against the bacteria *Escherichia coli* and *Methicillin-resistant Staphylococcus aureus*, as well as the fungi *Candida albicans* and *Candida parapsilosis*.

2. Experimental section

2.1. General details

All chemicals and solvents were used as supplied from commercial sources without further purification or drying, unless otherwise specifically stated in synthesis methods. The melting points of the corresponding compounds were measured using a Stuart™ melting point apparatus SMP10, AC input 230 V and were uncorrected. ^{1}H, ^{13}C, ^{19}F and ^{31}P NMR spectra were obtained at room temperature on a Varian VnmrS 400 MHz spectrometer. All NMR data was collected using $CDCl_3$ as the deuterated solvent which contains 0.03% (v/v) TMS. ^{1}H NMR chemical shifts were referenced to TMS; ^{19}F and ^{31}P chemical shifts were relatively referenced from the corresponding ^{1}H spectrum for the respective compounds. Total elemental analysis was undertaken using an Exeter Analytical CE-440 elemental analyser. Infrared spectra were obtained using a Bruker ALPHA Platinum ATR spectrometer. Crystal data for complexes **7–10** and **12** were collected using a Rigaku Oxford Diffraction (former Agilent Technologies, former Oxford Diffraction) SuperNova A diffractometer. All five were measured with Cu-Kα (λ = 1.54184 Å). A complete dataset was collected, assuming that the Friedel pairs are not equivalent. An analytical absorption correction, based on the shape of the crystal, was performed [35]. The structures were solved by direct methods using SHELXS [36] and refined by full matrix least-squares on F2 for all data using SHELXL [36]. Hydrogen atoms were added at calculated positions and refined using a riding model. Their isotropic temperature factors were fixed to 1.2 times the equivalent isotropic displacement parameters of the parent atom. Anisotropic thermal displacement parameters were used for all non-disordered non-hydrogen atoms. Analysis of cell culture plates for antibacterial testing was undertaken using a BioTek, Synergy HT plate reader. Analysis of cell culture plates for antifungal testing was undertaken every 15 min by a SynergyTM HT plate reader (BioTek Instruments, Inc., USA).

All silver carboxylates (**1–4**) and triphenylphosphino silver(I) benzoate complexes (**5–8**) were synthesized using adjusted synthesis methods [26,27]. All NHC*-silver(I) benzoate complexes were synthesized through the generation of a free carbene *via* the Arduengo method [28].

2.2. Synthesis of silver benzoates (*1–4*)

2.2.1. Silver benzoate (*1*)

Benzoic acid (0.488 g, 3.00 mmol) and silver(I) oxide (0.463 g, 2.00 mmol) were placed in 30 mL acetonitrile in a light proof flask and stirred for 24 h. The product was filtered *in vacuo*, washed with 30 mL acetonitrile and dried for 4 h to retrieve a grey solid (0.540 g, 79% yield).

^{1}H NMR (399.89 MHz, DMSO-d_6, ppm): 7.12–7.08 (2H, m, $CH_{Aromatic}$), 6.60–6.49 (2H, m, $CH_{Aromatic}$).

^{13}C NMR (100.55 MHz, DMSO-d_6, ppm): 170.7, 137.2, 130.5, 129.9, 128.1.

IR (ATR): 3049 (w, v), 1586 (m), 1375 (s), 715 (s), 675 (m), 443 (m).

Melting point: 280 °C.

Elemental Analysis calculated for $C_7H_5AgO_2$: Calculated: C, 36.71; H, 2.20; Found: C, 36.00; H, 2.51.

2.2.2. Silver 2-fluoro-benzoate (*2*)

2-Fluorobenzoic acid (0.560 g, 3.00 mmol) and silver(I) oxide (0.463 g, 2.00 mmol) were placed in 50 mL acetonitrile in a light proof flask and stirred for 24 h. The product was filtered *in vacuo* and washed with 10 mL acetonitrile. The solvent was removed and product dried under reduced pressure before being extracted and washed with 20 mL diethyl ether. Product was dried for 4 h to retrieve a grey solid. (0.824 g, 83% yield).

^{1}H NMR (399.89 MHz, DMSO-d_6, ppm): 7.69 (1H, td, J = 8, 2 Hz, $CH_{Aromatic}$), 7.42–7.32 (1H, m, $CH_{Aromatic}$), 7.18–7.06 (2H, m, $CH_{Aromatic}$).

^{13}C NMR (100.55 MHz, DMSO-d_6, ppm): 168.4, 161.87, 131.8, 131.7, 131.4, 131.3, 124.1, 124.0, 116.6, 116.3.

^{19}F NMR (376.24 MHz, DMSO-d_6, ppm): −112.4.

IR (ATR): 3075 (w, v), 1610 (m), 1586 (m), 1552 (m), 1523 (m), 1447 (m), 1376 (s), 1155 (m), 1090 (m), 857 (m), 747 (s), 657 (m), 545 (w), 446 (w).

Melting point: 230 °C.

Elemental Analysis calculated for $C_7H_4AgO_2F$: Calculated: C, 34.04; H, 1.62; Found: C, 34.20; H, 1.50.

2.2.3. Silver 3-fluoro-benzoate (*3*)

3-Fluorobenzoic acid (0.560 g, 3.00 mmol) and silver(I) oxide (0.463 g, 2.00 mmol) were placed in 50 mL acetonitrile in a light proof flask and stirred for 24 h. The product was filtered *in vacuo* and washed with 20 mL acetonitrile before being washed with 20 mL diethyl ether. Product was dried for 4 h to retrieve a grey solid. (0.635 g, 64% yield).

^{1}H NMR (399.89 MHz, DMSO-d_6, ppm): 7.75 (1H, dt, J = 8, 1 Hz, $CH_{Aromatic}$), 7.59 (1H, ddd, J = 10, 3, 1.5 Hz, $CH_{Aromatic}$), 7.39 (1H, td, J = 8, 6 Hz, $CH_{Aromatic}$), 7.28–7.17 (1H, m, $CH_{Aromatic}$).

^{13}C NMR (100.55 MHz, DMSO-d_6, ppm): 169.2, 163.4, 161.0, 140.4, 130.1, 130.0, 125.9, 125.8, 117.3, 117.0, 116.2, 116.0.

^{19}F NMR (376.24 MHz, DMSO-d_6, ppm): −114.1.

IR (ATR): 3087 (w,v), 1561 (m), 1376 (s), 1223 (m), 790 (m), 761 (s), 437 (m).

Melting point: 250 °C.

Elemental Analysis calculated for $C_7H_4AgO_2F$: Calculated: C, 34.04; H, 1.62; Found: C, 33.55; H, 1.47.

2.2.4. Silver 4-fluoro-benzoate (*4*)

4-Fluorobenzoic acid (0.841 g, 6.00 mmol) and silver(I) oxide (0.695 g, 3.00 mmol) were placed 50 mL acetonitrile and stirred for 24 h. The product was filtered *in vacuo* and washed with 20 mL acetonitrile before being washed with 20 mL diethyl ether. Product was dried for 4 h to retrieve a grey solid. (1.330 g, 90% yield).

^{1}H NMR (399.89 MHz, DMSO-d_6, ppm): 8.00–7.94 (2H, m, $CH_{Aromatic}$), 7.15 (2H, t, J = 9.0 Hz, $CH_{Aromatic}$).

^{13}C NMR (100.55 MHz, DMSO-d_6, ppm): 169.6, 165.1, 162.7, 133.9, 132.4, 132.3, 114.9, 144.7.

^{19}F NMR (376.24 MHz, DMSO-d_6, ppm): −111.99.

IR (ATR): 3068 (w, v), 1604 (m), 1499 (m), 1374 (s), 1229 (m), 1155 (m), 852 (m), 771 (s), 688 (m), 619 (s), 503 (w), 410 (w).

Melting point: 220 °C.

Elemental Analysis calculated for $C_7H_4AgO_2F$: Calculated: 34.04; H, 1.62; Found: C, 33.35; H, 1.44.

2.3. Synthesis of Triphenylphosphino-silver(I) benzoate complexes (**5**–**8**)

2.3.1. Bis-triphenylphosphino-silver(I) benzoate (**5**)

Triphenylphosphine (0.524 g, 2.00 mmol) and silver benzoate (0.229 g, 1.00 mmol) were dissolved in 20 mL of dry dichloromethane. The mixture was stirred in the absence of light for 2 d under nitrogen. The product was filtered *in vacuo* and washed with 20 mL of dry dichloromethane. The filtrate was concentrated to 2 mL and 5 mL of pentane was added. The product was extracted and dried for 4 h *in vacuo* to retrieve a white solid (0.596 g, 79% yield).

^{1}H NMR (399.89 MHz, $CDCl_3$, ppm): 8.14 (4H, dd, J = 8.3, 1.2 Hz, $CH_{Aromatic}$), 7.53–7.48 (10*H*, m, $CH_{Aromatic}$), 7.47 (10*H*, d, J = 3 Hz, $CH_{Aromatic}$), 7.46–7.41 (8H, m, $CH_{Aromatic}$), 7.41–7.38 (3H, m, $CH_{Aromatic}$).

^{13}C NMR (100.55 MHz, $CDCl_3$, ppm): 175.1, 134.6, 134.0, 133.8, 131.3, 131.2, 130.8, 130.0, 129.9, 129.5, 129.3, 129.2, 127.5.

^{31}P NMR (282.11 MHz, $CDCl_3$), ppm): 29.06.

IR (ATR): 3100 (w), 2900 (w), 1592 (m), 1537 (m), 1434 (m), 1305 (m), 1131 (w), 1095 (m), 691 (s), 489 (m).

Melting Point: 62 °C.

Elemental Analysis calculated for $C_{43}H_{35}AgO_2P_2$: C, 68.53; H, 4.68; A. Found: C, 68.25; H, 4.17.

2.3.2. Triphenylphosphino silver(I) 2-fluorobenzoate (**6**)

Triphenylphosphine (0.262 g, 1.00 mmol) and 2-fluoro-silver benzoate (0.247 g, 1.00 mmol) were dissolved in 5 mL of dry dichloromethane. The mixture stirred in the absence of light for 2 d under nitrogen. The product was filtered *in vacuo* and washed with 20 mL of dry dichloromethane. The filtrate was concentrated to 2 mL and 5 mL of pentane was added. The product was extracted and dried for 4 h *in vacuo* to retrieve a light brown solid (0.342 g, 70% yield).

^{1}H NMR (399.89 MHz, $CDCl_3$, ppm): 7.85 (1H, td, J = 7.5, 2 Hz, $CH_{Aromatic}$), 7.48–7.37 (10*H*, m, $CH_{Aromatic}$), 7.32 (7H, t, J = 7 Hz, $CH_{Aromatic}$), 7.12–7.03 (1H, m, $CH_{Aromatic}$).

^{13}C NMR (100.55 MHz, $CDCl_3$, ppm): 171.5, 162.4, 159.9, 134.0, 133.8, 130.8, 130.7, 130.3, 128.9, 128.8, 123.2, 123.3, 116.3, 115.9.

^{19}F NMR (376.24 MHz, $CDCl_3$, ppm): −113.26.

^{31}P NMR (282.11 MHz, CDC_{l3}), ppm): 11.22

IR (ATR): 3050 (w, v), 1591 (w), 1554 (w), 1476 (m), 1433 (m), 1370 (m), 1093 (m), 854 (m), 795 (s), 691 (s), 654 (s), 542 (s), 503 (s).

Melting Point: 110 °C.

Elemental Analysis calculated for $C_{25}H_{19}AgO_2FP$: C, 58.96; H, 3.76; Found: C, 58.78; H, 3.69.

2.3.3. Bis-triphenylphosphino silver(I) 2-fluorobenzoate (**7**)

Triphenylphosphine (0.524 g, 2.00 mmol) and 2-fluoro-silver benzoate (0.247 g, 1.00 mmol) were dissolved in 30 mL of dry dichloromethane. The mixture was stirred in the absence of light for 2 d under nitrogen. The product was filtered *in vacuo* and washed with 20 mL of dry dichloromethane. The filtrate was concentrated to 2 mL and 30 mL of pentane was added. The product was extracted and dried for 4 h *in vacuo* to retrieve a silver solid (0.713 g, 93% yield).

^{1}H NMR (399.89 MHz, $CDCl_3$, ppm): 7.77 (1H, td, J = 7.5, 2 Hz, $CH_{Aromatic}$), 7.48–7.33 (16H, m, $CH_{Aromatic}$), 7.29 (15H, t, J = 7.5 Hz, $CH_{Aromatic}$), 7.10 – 7.00 (2H, m, $CH_{Aromatic}$).

^{13}C NMR (100.55 MHz, $CDCl_3$, ppm): 171.1, 162.2, 134.0, 133.8, 132.5, 132.2, 131.6, 131.5, 130.2, 130.1, 130.0, 128.8, 128.7, 123.2, 123.1, 116.0, 115.8.

^{19}F NMR (376.24 MHz, $CDCl_3$, ppm): −113.83.

^{31}P NMR (282.11 MHz, $CDCl_3$), ppm): 8.74.

IR (ATR): 3049 (w, v), 1591 (m), 1555 (m), 1478 (m), 1433 (m), 1371 (m), 1026 (m), 854 (m), 741 (s), 690 (s), 501 (s).

Melting Point: 140 °C.

Elemental Analysis calculated for $C_{43}H_{34}O_2AgFP_2$: C, 66.93; H, 4.44; Found: C, 66.60H, 5.33.

2.3.4. Bis-triphenylphosphino silver(I) 4-fluorobenzoate (**8**)

Triphenylphosphine (0.524 g, 2.00 mmol) and 4-fluoro-silver benzoate (0.247 g, 1.00 mmol) were dissolved in 20 mL of dry dichloromethane. The mixture was stirred in the absence of light for 2 d under nitrogen. The product was filtered *in vacuo* and washed with 20 mL of dry dichloromethane. The filtrate was concentrated to 2 mL and 5 mL of pentane was added. The product was extracted and dried for 4 h *in vacuo* to retrieve a light brown solid (0.650 g, 84% yield).

^{1}H NMR (399.89 MHz, $CDCl_3$, ppm): 8.11–8.02 (2H, m, $CH_{Aromatic}$), 7.44–7.32 (19H, m, $CH_{Aromatic}$), 7.27 (6H, s, $CH_{Aromatic}$), 7.24 (5H, d, J = 7 Hz, $CH_{Aromatic}$), 7.04–6.95 (2H, m, $CH_{Aromatic}$).

^{13}C NMR (100.55 MHz, $CDCl_3$, ppm): 173.1, 164.9, 162.4, 133.0, 132.8, 131.3, 131.2, 131.1, 130.9, 130.3, 130.3, 130.0, 130.0, 129.0, 128.6, 128.4, 128.3, 127. 5, 127.4, 113.8, 113.6.

^{19}F NMR (376.24 MHz, $CDCl_3$, ppm): −112.72.

^{31}P NMR (282.11 MHz, $CDCl_3$), ppm): 8.56.

IR (ATR): 3100 (w, v), 1606 (m), 1555 (m), 1478 (m), 1434 (m), 1370 (m), 1215 (m), 1146 (m), 1095 (m), 856 (m), 780 (7 8 0), 742 (s), 692 (s), 611 (s), 495 (s).

Melting Point: 152 °C.

Elemental Analysis calculated for $C_{43}H_{34}O_2AgFP_2$: C, 66.93; H, 4.44; Found: C, 67.16; H, 4.70.

2.4. Synthesis of 1,3-dibenzyl-4,5-diphenyl imidazol-2-ylidene silver(I) benzoate complexes (**9**–**12**)

1 mL of 1 M potassium *tert*-butoxide solution (1.00 mmol) was injected at 0 °C to a mixture of 30 mL dry tetrahydrofuran and 1,3-dibenzyl-4,5-diphenyl imidazolium bromide (0.481 g, 1.00 mmol), under nitrogen. The reaction was stirred for 1 h at room temperature and allowed to settle for 30 min. The solution was syringed from the reaction flask and injected into a second flask containing 30 mL dry tetrahydrofuran and 1.00 mmol of the corresponding silver benzoate; all additions are kept under nitrogen. The reaction mixture was stirred for 3 d under nitrogen. The reaction mixture was filtered *in vacuo* and re-filtered using a grade 4 sinter funnel. The filtrate was removed under reduced pressure to retrieve a solid that was dissolved in chloroform and filtered using a grade 4 sinter funnel. The filtrate was filtered by gravity filtration to remove remaining impurities and concentrated to 3 mL under reduced pressure. 80 mL of pentane was added and the solution was allowed to sit for 24 h. The solid product was extracted with pentane, filtered *in vacuo* and dried for 4 h.

2.4.1. Synthesis of 1,3-dibenzyl-4,5-diphenyl imidazol-2-ylidene silver(I) benzoate (**9**)

20 mL of the carbene/THF solution is injected into a reaction flask containing silver benzoate (0.228 g, 1.00 mmol) in 30 mL tetrahydrofuran at room temperature, whilst stirring. The reaction is stirred for 3 d and worked up to achieve a brown solid (0.207 g, 33% yield).

^{1}H NMR (399.89 MHz, $CDCl_3$, ppm): 8.10 (2H, d, J = 8 Hz, $CH_{Aromatic}$), 7.44–7.34 (3H, m, $CH_{Aromatic}$), 7.28 (2H, t, J = 7.5 Hz, $CH_{Aromatic}$), 7.24–7.19 (9H, m, $CH_{Aromatic}$), 7.03–6.96 (8H, m, $CH_{Aromatic}$), 5.38 (4H, s, $CH2_{Benzyl}$).

^{13}C NMR (100.55 MHz, $CDCl_3$, ppm): 179.7, 173.4, 136.1, 132.7, 130.6, 130.4, 129.5, 129.1, 128.6, 128.5, 127.9, 127.7, 127.3, 53.7.

IR (ATR): 3058 (w), 1596 (w), 1565 (w), 1442 (w), 1365 (m), 1020 (w), 836 (w), 838 (w), 761 (w), 722 (m), 696 (s), 614 (w), 579 (w), 519 (w), 453 (w).

Melting point: 176 °C.

Elemental Analysis calculated for $C_{36}H_{29}N_2AgO_2$: Calculated: C, 68.69; H, 4.64; N, 4.45; Found: C, 68.13; H, 4.56; N, 4.23.

2.4.2. Synthesis of 1,3-dibenzyl-4,5-diphenyl imidazol-2-ylidene silver(I) 2-fluorobenzoate (**10**)

20 mL of the carbene/THF solution is injected into a reaction flask containing 2-fluoro-silver benzoate (0.247 g, 1.00 mmol) and 30 mL tetrahydrofuran at room temperature, whilst stirring. The reaction is stirred for 3 d and worked up to achieve a silver solid (0.359 g, 55% yield).

^{1}H NMR (399.89 MHz, $CDCl_3$, ppm): 7.95–7.89 (1H, m, $CH_{Aromatic}$), 7.32–7.26 (3H, m, $CH_{Aromatic}$), 7.25–7.18 (9H, m, $CH_{Aromatic}$), 7.12–7.06 (2H, m, $CH_{Aromatic}$), 7.05–6.97 (9H, m, $CH_{Aromatic}$), 5.37 (4H, s, $CH2_{Benzyl}$).

^{13}C NMR (100.55 MHz, $CDCl_3$, ppm): 179.3, 170.8, 162.7, 160.2, 136.2, 132.7, 132.5, 131.7, 131.6, 130.6, 129.1, 128.7, 128.5, 128.0, 127.6, 127.3, 123.4, 116.4, 116.1, 53.7.

^{19}F NMR (376.24 MHz, $CDCl_3$, ppm): −112.2.

IR (ATR): 3058 (w), 1595 (m), 1549 (m), 1449 (m), 1374 (s), 1218 (m), 857 (m), 757 (s), 735 (m), 698 (s), 656 (m), 461 (w).

Melting point: 154 °C.

Elemental Analysis calculated for $C_{36}H_{28}N_2AgO_2F$: Calculated: C, 66.78; H, 4.36; N, 4.33; Found: C, 66.65; H, 4.25; N, 4.20.

Synthesis of 1,3-dibenzyl-4,5-diphenyl imidazol-2-ylidene silver(I) 3-fluorobenzoate (**11**).

20 mL of the carbene/THF solution is injected into a reaction flask containing 3-fluoro silver benzoate (0.247 g, 1.00 mmol) and 30 mL tetrahydrofuran at room temperature, whilst stirring. The reaction is stirred for 3 d and worked up to achieve a light brown solid (0.129 g, 19% yield).

^{1}H NMR (399.89 MHz, $CDCl_3$, ppm): 7.87 (1H, d, J = 7.5 Hz, $CH_{Aromatic}$), 7.78 (1H, d, J = 10 Hz, $CH_{Aromatic}$), 7.30 (3H, dd, J = 16, 8.5 Hz, $CH_{Aromatic}$), 7.23 (10*H*, dd, J = 5.5, 2.0 Hz, $CH_{Aromatic}$), 7.10 (1H, t, J = 8.5 Hz, $CH_{Aromatic}$), 7.00 (8H, d, J = 7 Hz, $CH_{Aromatic}$), 5.38 (4H, s, CH_{Benzyl}).

^{13}C NMR (100.55 MHz, $CDCl_3$, ppm): 179.6, 163.7, 136.1, 132.7, 130.6, 129.1, 128.7, 128.69, 128.5, 128.0, 127.6, 127.3, 125.5, 117.3, 117.1, 53.7.

^{19}F NMR (376.24 MHz, $CDCl_3$, ppm): −114.3.

IR (KBr, cm-1): 3053 (w), 1602 (w), 1571 (m), 1438 (w), 1357 (m), 1222 (w), 795 (m), 767 (s), 696 (s), 614 (w), 444 (w).

Melting point: 164 °C.

Elemental Analysis calculated for $C_{36}H_{28}N_2AgO_2F$: Calculated: C, 66.78; H, 4.36; N, 4.33; Found: C, 66.26; H, 4.22; N, 4.24.

2.4.3. Synthesis of 1,3-dibenzyl-4,5-diphenyl imidazol-2-ylidene silver(I) 4-fluorobenzoate (**12**)

20 mL of the carbene/THF solution is injected into a reaction flask containing 4-fluoro silver benzoate (0.247 g, 1.00 mmol) and 30 mL tetrahydrofuran at room temperature, whilst stirring. The reaction is stirred for 3 d and worked up to achieve a light brown solid (0.311 g, 48% yield).

^{1}H NMR (399.89 MHz, $CDCl_3$, ppm): 8.10 (2H, dd, J = 9, 6 Hz, $CH_{Aromatic}$), 7.29 (2H, t, J = 7.5 Hz, $CH_{Aromatic}$), 7.25–7.19 (10*H*, m, $CH_{Aromatic}$), 7.06–6.97 (10*H*, m, $CH_{Aromatic}$), 5.38 (4H, s, $CH2_{Benzyl}$).

^{13}C NMR (100.55 MHz, $CDCl_3$, ppm): 179.6, 172.7, 166.6, 163.1, 136.1, 132.7, 132.1, 132.0, 130.6, 129.1, 128.6, 128.5, 128.0, 127.6, 127.3, 114.5, 114.3, 53.8.

^{19}F NMR (376.24 MHz, $CDCl_3$, ppm): −111.1.

IR (ATR): 3056 (w,v), 1616 (w), 1584 (w), 1344 (m), 1209 (w), 1147 (w), 856 (m), 742 (m), 697 (s), 623 (m), 479 (w).

Melting point: 207 °C.

Elemental Analysis calculated for $C_{36}H_{28}N_2AgO_2F$: Calculated: C, 66.78; H, 4.36; N, 4.33; Found: C, 66.41; H, 4.38; N, 4.14.

2.5. Antimicrobial studies

2.5.1. Kirby-Bauer Disk Diffusion

In vitro screening for antibacterial efficacy was conducted using the Kirby-Bauer Disk Diffusion method against one Gram-positive pathogenic bacterial strain and one Gram-negative pathogenic bacterial strain; *Methicillin-resistant Staphylococcus aureus* (ATCC43300) was chosen as the Gram-positive strain and *Escherichia coli* (ATCC 25922) was chosen as the Gram-negative strain [25].

Both bacterial strains were cultured in 2 mL LB medium from single colonies at 37 °C for 24 h whilst shaking. 50 µL of culture was spread over agar-LB medium (SIGMA *L2897*) in a petri plate and to each plate 5.5 mm Whatman paper disks were evenly placed into four marked quadrants. Stock solutions of the silver benzoate starting materials (**1–4**) and silver complexes (**5–12**) were made to a 1 mg/mL dilution in DMSO. Two volumes of 5 µL and 10 µL were tested for each silver benzoate and complex against both bacterial strains. DMSO, without the addition of a silver complex, was used as a control in 5 µL and 10 µL volumes; three other antibacterial compounds were also used in 1 mg/ml dilutions as comparative controls. All plates were incubated at 37 °C for 24 h. The area of clearance is defined as the distance between the beginning of bacterial growth and the edge of the Whatman disk; the zone of inhibition (radius) was measured in millimetres (mm). All antibacterial work was carried out under sterile conditions [32]. Single run assays performed, no replicates were conducted as this was used as a preliminary screening of antibiotic activity.

2.5.2. Minimum Inhibitory Concentration (MIC) – bacterial assays

Further *in vitro* screening against bacteria was conducted on the two most potent complexes against *Methicillin-resistant Staphylococcus aureus* (ATCC43300). The *MRSA* strain was cultured to the stationary phase (OD_{600} = 2) in nutrient broth (OXOID *CM0001*) for 24 h at 37 °C, whilst shaking.

To a 96-well cell culture plate (Sarstedt), 100 µL of nutrient broth was added to each well. 1 mg/mL dilutions of complexes **8** and **12** were made in DMSO, which was further diluted to a 10% DMSO solution in deionised water. A 10% DMSO/water solution and a SBC3 NHC-silver (I) acetate complex [22] solution in 10% DMSO/water were tested simultaneously as comparative controls. 100 µL of the stock silver complex solutions were added to respective plates and a serial dilution was carried out to give a concentration range of 0.39–100 µg/mL. 100 µL of the *MRSA* cell suspension was added to the cell culture plates and the plates then incubated for 24 h at 37 °C The plates were measured for effect of inhibition using a microplate reader (BioTek, Synergy HT) at OD_{570} and all growth is presented as a percentage of the control. All assays were performed in triplicate [24].

2.5.3. Minimum Inhibitory Concentration (MIC) – fungal assays

In vitro screening against fungi was conducted on all silver complexes (**5–12**) to determine the extent of broad spectrum activity. Preliminary testing was carried out on cells growing in minimal media to establish the effectiveness of both classes of silver complexes, and the MIC values were determined using the CSLI standard method [34]. Complexes were tested against the two pathogenic fungi *Candida albicans* SC5314 and *Candida parapsilosis* CLIB214 (ATCC22019).

For growth inhibition assays, complexes (**5–12**) were freshly made to a 2 mg/mL concentration in ethanol, and a serial dilution was performed to the desired concentration range (0.15625–40 µg/mL) in 100 µL in a U-bottom 96-well (Sarstedt) plate. Both yeast species were maintained on YPD (1% Yeast extract, 2% Peptone and 2%Dextrose) agar plates and a single colony was inoculated to 5 mL YPD broth medium and grown overnight at 30 °C with shaking. Yeast cells were collected and re-suspended in Yeast Nutrient Broth (YNB: 0.19% Yeast

nitrogen base without amino acids and without ammonium sulfate (Formedium, CYN0501), 0.5% ammonium sulfate (Sigma, A4418), 0.079% amino acids (Formedium, DCS0019) and 2% glucose) to an optical density (A_{600}) of 0.02. 100 µL of yeast inoculum was loaded on top of the 100 µL drug dilutions. The A_{600} of the plate was read every 15 min for 24 h by using a SynergyTM HT plate reader (BioTek Instruments, Inc., USA) and recorded using the Gen5TM Microplate Software (BioTek Instruments, Inc., USA). All results are expressed as a % growth compared to the growth of the control. All assays were replicated in quadruplicate.

The MIC values of complexes **9–12** were determined using the standardized broth microdilution method as recommended by the CLSI document M27-A3 (CLSI, 2008) [34]. All compounds were freshly prepared and diluted to 40 µg/mL, 20 µg/mL, 10 µg/mL, 5 µg/mL, 2.5 µg/mL, 1.25 µg/mL, 0.625 µg/mL, 0.3 µg/mL and 0.15 µg/mL. Inocula were prepared from a 24 h culture on Sabouraud Dextrose agar plate, adjusted to same absorbance of the 0.5 Mac Farland standard (CLSI, M27-S3) at 530 nm, and diluted in RPMI-1640 (Sigma, R1383) supplemented with 0.02% glucose (Sigma, G8720) to the desired concentration of 1–5 × 103 colony-forming units (CFU)/ml. 100 µL of drug dilution was mixed with 100 µL of inoculum in a U-bottom 96-well plate and incubated at 35 °C. Plates were scored at 24 h and 48 h. The MIC was defined as the lowest concentration of drug that inhibits 50% growth relative to the growth in the drug-free control well after 48 h. Commercial antifungal drugs Fluconazole (Sigma, F8929) and Caspofungin (Sigma, SML0425) were tested against *C. albicans* SC5314, *C. parapsilosis* CLIB214 (ATCC22019) and *C. krusei* (ATCC6258), with the later two as references recommended by CLSI to confirm the accuracy of the assays. All assays were replicated in quadruplicate.

3. Results & discussion

3.1. Synthesis

The synthesis of the silver carboxylates (**1–4**) was achieved using a modified literature method to produce the silver benzoate and three fluorinated silver benzoates species [26] (Scheme 1). The benzoic acid starting materials were reacted with silver oxide in acetonitrile, in the absence of light, to retrieve the corresponding silver benzoates (Scheme 1). The products were obtained in good yields (64–83%) with high purity using the stated work-up.

The corresponding benzoates were used as starting materials for the synthesis of the respective combination triphenylphosphino– and NHC*-silver(I) complexes. Complexes **5–8** were synthesized using a modified literature method [27] (Scheme 2), with an intermediate free carbene generated during the synthesis of complexes **9–12** [28] (Scheme 3). For complex **6**, the 2-fluoro-silver benzoate was reacted with 1 equivalent of triphenylphosphine for 2 d in dried dichloromethane, in darkness and under nitrogen (Scheme 2). For the remaining triphenylphosphino-silver(I) benzoate complexes (**5**, **7**, **8**), the corresponding silver carboxylates were reacted with 2 equivalents of triphenylphosphine for 2 d in dry dichloromethane, in darkness and under nitrogen (Scheme 2).

The NHC*-carbene silver(I) benzoate complexes (**9–12**) were

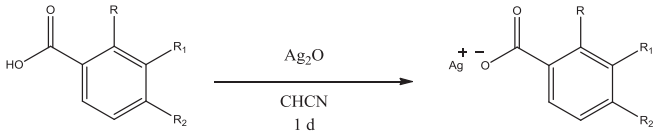

Scheme 1. Synthesis of silver benzoates **1–4**.

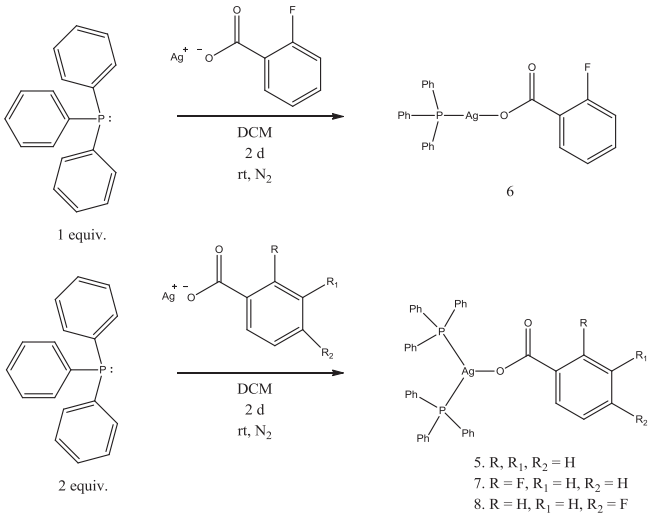

Scheme 2. Synthesis of triphenylphosphino-silver(I) benzoate complexes **5–8**.

synthesized by first generating a free carbene from the precursor imidazolium bromide salt [28], which was made in 80% yield using a modified literature method and confirmed by spectroscopic analysis [22,25].

Generation of the free carbene is achieved by injecting 1 mL of 1 M potassium *tert*-butoxide in THF solution into a flask charged with 1 mol of the imidazolium bromide and 30 mL dried THF, at 0 °C under nitrogen. After stirring for 1 h, the resulting reaction solution was then transferred to a secondary flask containing 1 equivalent of the corresponding silver benzoates (**1–4**) in 30 mL dried THF, under nitrogen. The reaction was stirred for 3 d at room temperature and worked up to achieve solid products in 19–55% yield (Scheme 3). The side product of potassium bromide is produced during the generation the free carbene and must be allowed to settle before the solution can be transferred to the secondary reaction flask. The use of a small reaction flask (50–100 mL) led to an increase in transferrable amount of the free carbene solution, resulting in higher yields.

3.2. Characterisation

The synthesis of the silver carboxylates (**1–4**) were all confirmed by IR spectroscopy, showing the loss of the distinctive wide carboxylic acid 'OH' band between 3000 and 2500 cm^{-1}, and by elemental analysis.

Complexes **5–8** were confirmed by NMR spectroscopy (^{1}H, ^{19}F, ^{31}P), IR spectroscopy and elemental analysis. All complexes integrated to the correct number of protons in ^{1}H NMR, with corresponding singlet signals observed at the correct ranges in both the ^{19}F spectra (−112 to −113 ppm) [29] and ^{31}P spectra (11–8 ppm) [27].

Complexes **9–12** were confirmed by NMR spectroscopy (^{1}H, ^{19}F), IR spectroscopy and elemental analysis. The loss of the carbene proton peak in the range of 10.50–11.50 ppm shows deprotonation of the NHC-ligand in ^{1}H NMR, and correct integration of the aromatic region was found for the additional 5 benzyl protons of benzoate **1** and 4 benzyl protons of benzoates **2–4**. Singlet signals were found in the correct ranges corresponding to benzyl fluorine groups (−111 to −114) in ^{19}F NMR [29]. ^{13}C NMR spectra for all complexes showed additional peaks in the range of 179.3–179.7 ppm which correspond to previous literature values for the carbene carbon after bonding with silver [22,30–34]; an additional signal is also seen for each complex between 170.8 and 173.4 ppm, which is accounting for the carbonyl carbon of the benzoate moiety.

IR spectroscopy revealed characteristic signals for all the NHC*-Ag-benzoates at 1374–1344 cm^{-1}, corresponding to the carboxylate carbonyl carbon-oxygen double bond, and at 1222–1209 cm^{-1} for the fluorinated species, corresponding to the carbon-fluorine bond.

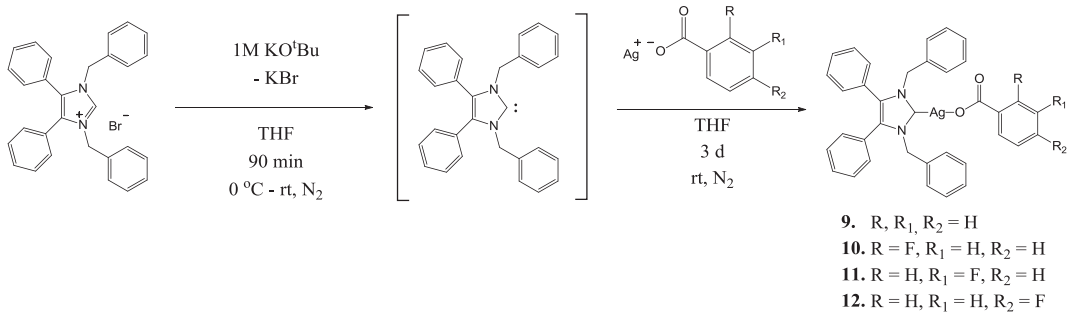

Scheme 3. Synthesis of NHC*-silver(I) benzoates complexes **9–12**.

Crystal structures were obtained for complexes **7**, **8**, **9**, **10** and **12**, with the structures for complexes **8** and **12** are presented in Fig. 7, as these complexes were chosen for further antibacterial testing. Crystal structures for complexes **7**, **9** and **10** can be seen in Fig. 8, with additional data for all structures found in the Supplementary information.

3.3. Biological results

Preliminary screening to indicate the antibacterial activity of the 8 new complexes **5–12** was carried out using the Kirby-Bauer Disk Diffusion method [25]. The following results can be seen in Figs. 2 and 3. The eight novel complexes were compared to the silver benzoates (**1–4**) and three control compounds of proven antibacterial activity (SBC3, Tetracycline and Ciprofloxacin).

Fig. 2 confirms that the proven antimicrobial compounds Tetracycline and Ciproflaxin are highly effective against *MRSA*, producing zones of clearance with a radius of 14 mm and 12 mm, respectively. The SBC3 molecule shows the next greatest efficacy with a 5 mm radius zone of clearance, whereas complexes **10** and **12** each show similar activity with a 4.5 mm radius zone of clearance. The triphenylphosphino-silver(I) benzoate complex **8** also shows similar activity to SBC3 with a zone of clearance of radius 4 mm. All compounds were tested by administering 10 µL volume of a 1 mg/mL solution of the compounds in DMSO.

Fig. 3 shows the effect of the tested compounds against *E. coli*. Again, Tetracycline and Ciprofloxacin show very good activity against the bacterium, producing 12 mm and 16 mm radius zones of clearance, respectively. SBC3 also shows some activity against *E. coli* with a 4 mm radius zone of clearance. Complexes **9**, **11** and **12** show similar activity to SBC3 with zones of clearance of radius 5–6 mm. However, against *E. coli* the triphenylphosphino-silver(I) benzoate complexes show little to no inhibition. This shows that, similar to the SBC3 molecule, the new NHC*-silver(I) benzoate complexes have broad spectrum activity against both Gram-negative and Gram-positive bacteria, showing a possible greater activity against Gram-negative bacteria in these preliminary tests. Measurements of zones of inhibition for all tested compounds can be found in the Supplementary information.

Two complexes were chosen for further *in vitro* screening to determine Minimum Inhibitory Concentration (MIC) [24,34]; one triphenylphosphino-silver(I) benzoate complex, **8**, and one NHC*-silver(I) benzoate complex, **12**. These complexes represented similar activity against *MRSA* and contained the same 4-fluoro-benzoate modality, and therefore both were tested to determine their MIC.

As can be seen in Fig. 4, all complexes inhibit growth in the higher concentration ranges (100–25 µg/mL). However, at 25 µg/mL complex **8** inhibits growth poorly. At all concentrations the inhibitory effect of complex **12** shows similar activity to the SBC3 molecule. At the 25 µg/mL concentration, SBC3 shows 79% inhibition of growth while complex **12** shows 65% inhibition of growth. Inhibition of *MRSA* stays at below 50% at a concentrate of 6.25 µg/mL or higher; similar to previous reported values for SBC3 against *Methicillin-susceptible Staphylococcus aureus* [24]. Complex **12** therefore has similar antibacterial properties to SBC3 and a possible greater effect against Gram-negative bacteria (Fig. 3). Detailed data of the antibacterial MIC testing can be found in the Supplementary information.

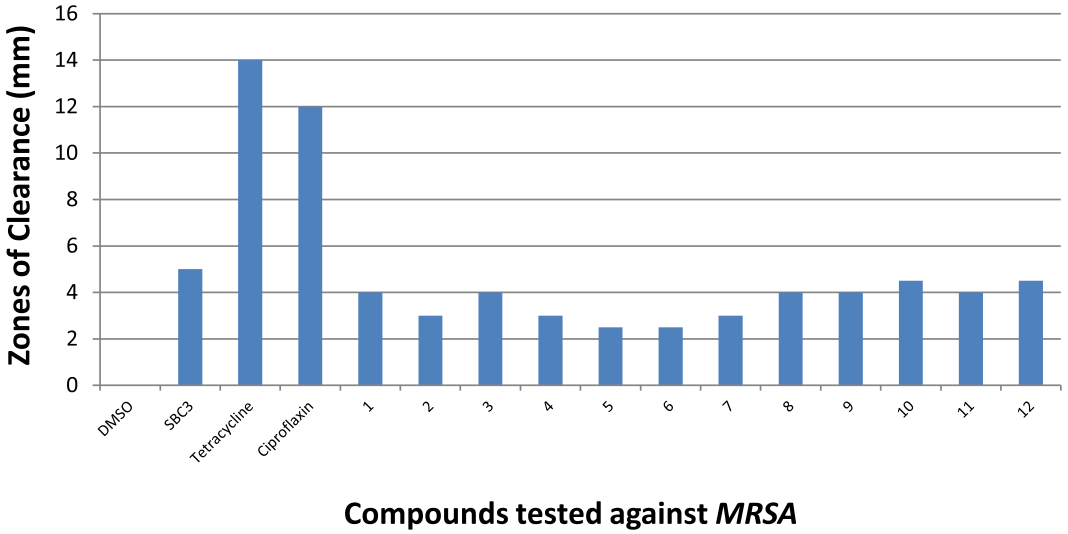

Fig. 2. Radius of zones of clearance (mm) against *MRSA* using 10 µL volume of 1 mg/mL DMSO/ silver(I) compounds (SBC3, **1–12**) solutions and 1 mg/mL DMSO/ compound (Tetracycline, Ciproflaxin) solutions.

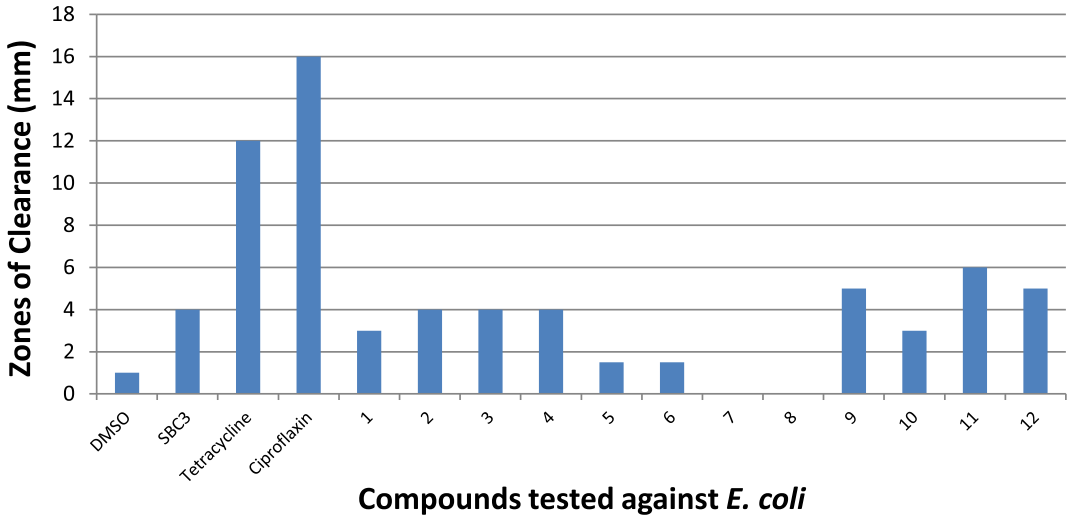

Fig. 3. Radius of zones of clearance (mm) against *E. coli* using 10 µL volume of 1 mg/mL DMSO/silver(I) compounds (SBC3, **1–12**) solutions and 1 mg/mL DMSO/compound (Tetracycline, Ciproflaxin) solutions.

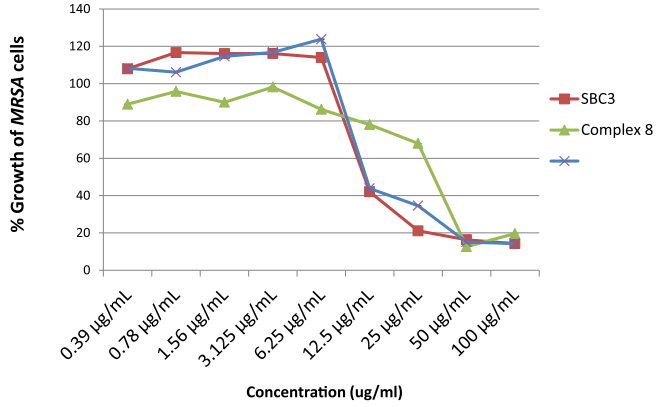

Fig. 4. Inhibition of *MRSA* growth by SBC and complexes **8** & **12**.

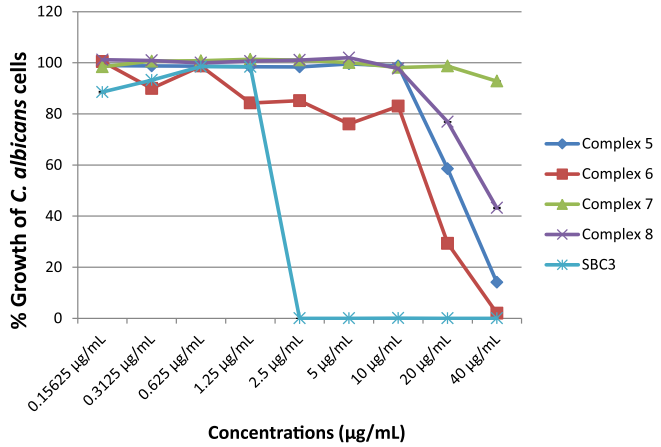

Fig. 5. Inhibition of *C. albicans* growth by triphenylphosphino-silver(I) benzoate complexes (**5–8**).

To determine the broad spectrum ability of the new complexes (**5–12**), antifungal activity was tested for against *Candida albicans* SC5314 and *Candida parapsilosis* CLIB214 (ATCC22019). Figs. 5 and 6 present and compare the activity of the triphenylphosphino-silver(I) benzoate complexes (**5–8**) with SBC3.

Fig. 5 shows that the triphenylphosphino-silver(I) benzoate complexes inhibit the growth of *C. albicans* when administered at higher concentrations, with complexes **5** and **6** inhibiting more than 80% growth at 40 µg/mL. In Fig. 6, complexes **5** and **6** show more than 80% inhibition at the 40 µg/mL concentration against *C. parapsilosis*. Complex **6** retains a greater than 80% inhibition at 20 µg/mL concentration, but complexes **5** and **8** show lessened activity of against *C. parapsilosis* at the lower concentration of 20 µg/mL. Complex **7** shows no inhibition greater than 40%.

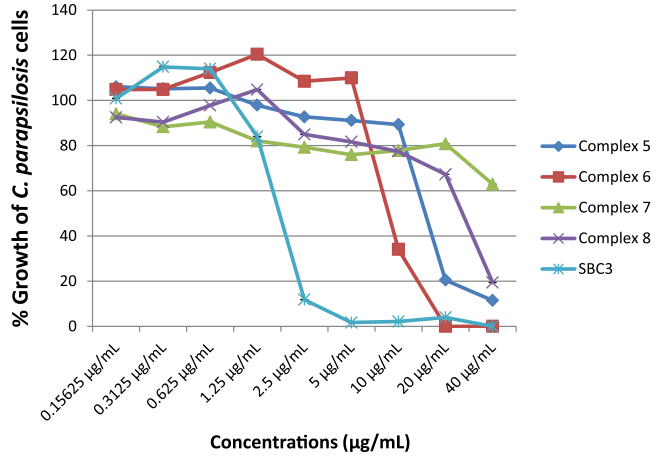

Fig. 6. Inhibition of *C. parapsilosis* growth by triphenylphosphino-silver(I) benzoate complexes (**5–8**).

For the NHC*-silver(I) benzoate complexes, **9–12**, the MIC against both *C. albicans* and *C. parapsilosis* was determined using the CLSI standardized broth microdilution method [34]. MIC was determined as the lowest concentration that causes 50% inhibition of growth.

Table 1 compares the MIC values for SBC3, complexes **9–12** and two antifungal standards (Fluconazole and Caspofungin) were used as internal references are presented; an additional control strain (*Candida krusei* ATCC6258) was also incorporated. The MICs of the two internal controls (Fluconazole and Caspofungin) lie within the expected ranges.

For SBC3 and complexes **9–12**, there are consistent MIC values at concentrations of 0.625 µg/mL against *C. albicans* and consistent MIC values at concentrations of 0.3125 µg/mL against *C. parapsilosis*. Whilst the MIC value of the silver(I) complexes is higher than that of Caspofungin and Fluconazole against *C. albicans*, these silver(I) complexes show inhibition at comparable concentrations to the two control compounds against *C. parapsilosis*.

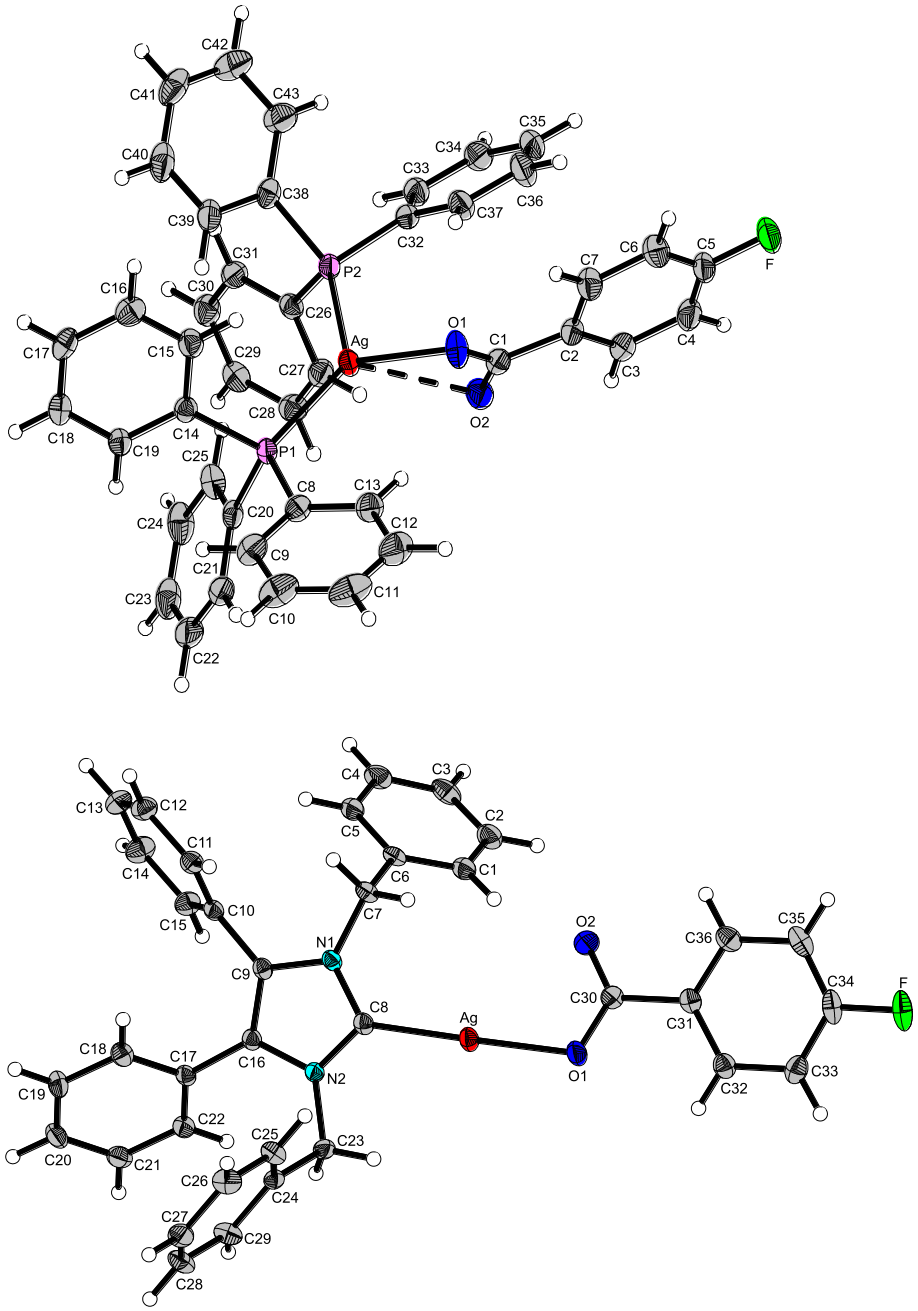

Fig. 7. Crystal structures of complex **8** and complex **12**; thermal ellipsoids are drawn on a 50% probability level for both structures.

3.4. Crystal structures

In Fig. 7 the structures of complexes **8** and **12** are presented. Both crystals were obtained by the slow diffusion of pentane into a saturated solution of the corresponding complexes in dichloromethane at -4°C. In complex **8**, the bond distances from the silver atom to both the triphenylphosphine phosphorus atoms and the benzoate oxygen are similar to previous literature values, as are bond angles between the silver, phosphorus and oxygen atoms [27] (Table 2).

Similarly, the bond lengths of the silver to both the NHC*-backbone and carboxylate oxygens of complex **12** show comparable bond distances to previously reported NHC*-silver(I) complexes by our group [22,30–33] (Table 2), despite the incorporation of the new benzoate group. However, in complex **12** the bond angle between the NHC, silver atom and carboxylate oxygen is more linear than previous NHC*-silver (I) complexes at an angle of 178.86(6)° [22,30–33]. Comparatively, complex **8** adopts an η^{1+1} coordination between the carboxylate oxygens, as the second interaction between the silver atom and the carbonyl oxygen has too great a distance to be considered a bond (2.724(2) pm), and can more correctly be characterised as a 'long contact' interaction. Complex **12** remains in η^1 coordination, despite the same fluorinated benzoate substituent in both of these complexes.

In Fig. 8, the structures for complexes **7**, **9** and **10** are presented. In the crystal structure of complex **7**, there is definitive η^2 bonding seen between both oxygens of the benzoate and silver atom, showing distances of similar lengths at 2.5559(13) and 2.4349(13) Å for both the silver-oxygen bonds, Ag–O(1) and Ag–O(2), respectively. Bond lengths and angles for the phosphorus-silver bond are also similar and consistent with complex **8** and literature values [27]. In the structures of complexes **9** and **10**, bond lengths for the carbene carbon bond to silver and silver to benzoate oxygen remain very similar to complex **12**. The major difference between these complexes is the less linear character of

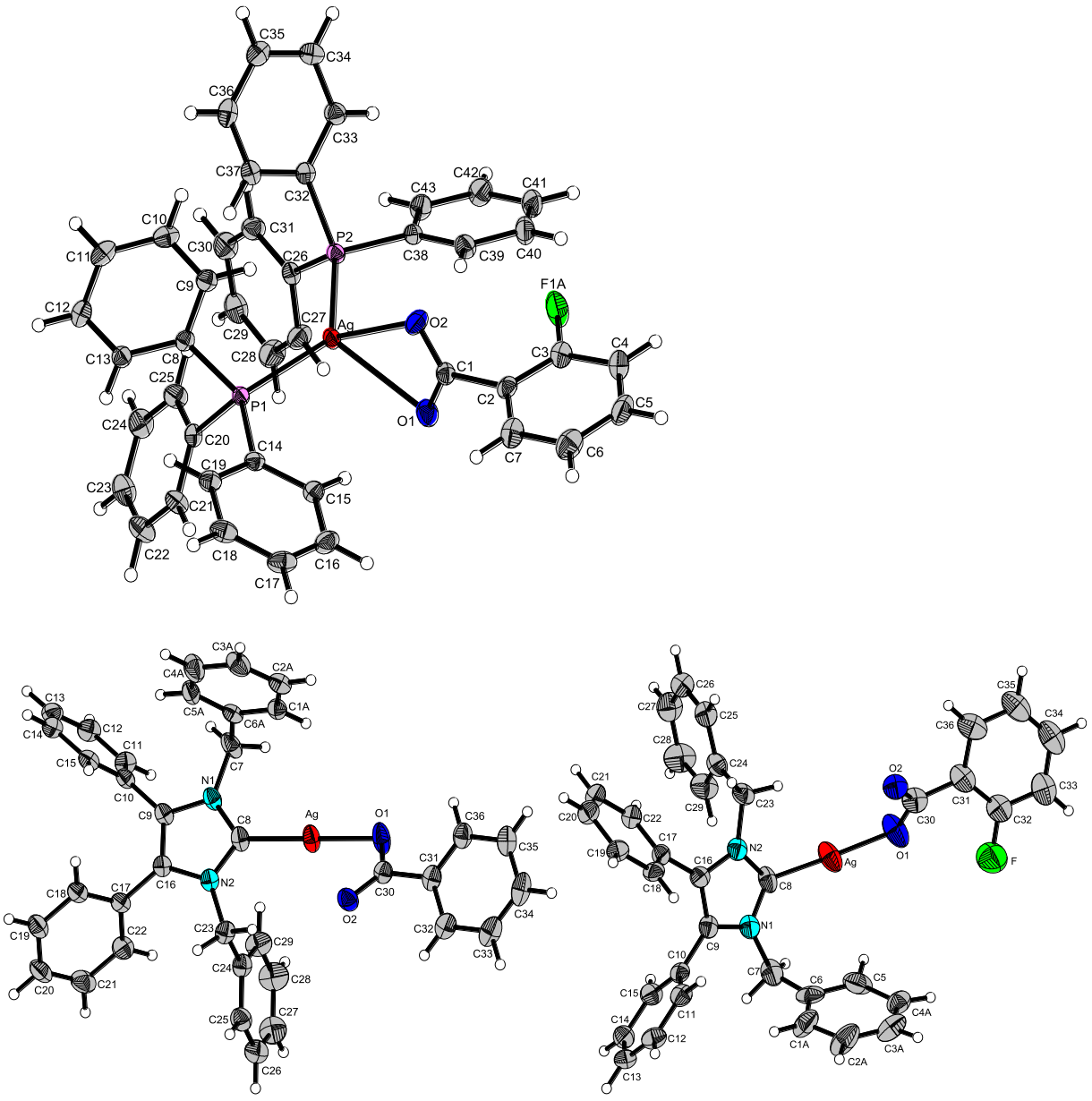

Fig. 8. Crystal structures of complexes **7**, **9** and **10**; thermal ellipsoids are drawn on a 50% probability level for all three structures.

Table 1
MIC values of complexes **9–12** against *C. albicans* and *C. parapsilosis* (NT = not tested).

MIC (μg/mL)			
	C. albicans SC5314	*C. parapsilosis* CLIB214	*C. krusei* ATCC6258
Fluconazole	0.125	0.5	16
Caspofungin	0.25	2	2
SBC3	0.625	0.3125	NT
9	0.625	0.3125	NT
10	0.625	0.3125	NT
11	0.625	0.3125	NT
12	0.625	0.3125	NT

Table 2
Selected bond lengths and angles for complexes **8** and **12**.

Bond length/Å	8	12
Ag–C(8)		2.0588(17)
Ag–O(1)		2.1038(12)
Ag–O(1)	2.3080(12)	
Ag–P(1)	2.4042(4)	
Ag–P(2)	2.4498(4)	
O(1)–C(1)	1.264(2)	
Bond angle/°		
C(8)-Ag-O(1)		178.86(6)
O(1)–Ag–P(1)	118.14(4)	
O(1)–Ag–P(2)	112.09(4)	
P(1)–Ag–P(2)	128.843(14)	

the bonding between the carbene carbon, the silver centre and the benzoate oxygen, which is calculated at 174.94(8)° and 175.60(17)° for complexes **9** and **10**, respectively. All crystallographic data can be found in the Supplementary information.

4. Conclusions

Four triphenylphosphino-silver(I) benzoate complexes and four 1,3-dibenzyl-4,5-diphenyl imidazol-2-ylidene silver(I) benzoate complexes,

were successfully synthesised from either triphenylphosphine or the free NHC* ligand. Their biological activity was evaluated against *MRSA*, *E. coli*, *C. albicans* and *C. parapsilosis* allowing to identify antibiotic drug candidates.

Against the bacterial strains, all complexes induce some inhibitory effect in Kirby-Bauer Disk Diffusion testing against *MRSA*, with the NHC*-silver(I) benzoate complexes showing the most promising antibacterial activity. In the Kirby-Bauer testing, all NHC*-silver(I) benzoate complexes **9–12** show equal activity to the SBC3 molecule against the Gram-positive bacteria *MRSA* and against the Gram-negative bacteria *E. coli*, demonstrating broad spectrum activity equal to SBC3. The NHC*-silver(I) benzoate complex **12** also completely inhibits growth at a concentration of 12.5 μg/mL, similar to that of SBC3 against *MRSA*.

The antifungal activity of complexes **5–12** against *C. albicans* and *C. parapsilosis* was also determined. Preliminary testing was conducted using a similar method to that of the antibacterial testing, and the MICs of complexes **9–12** were determined by retesting and using the CLSI standardized broth microdilution method. These results showed that SBC3 and all the NHC*–silver(I) benzoate complexes had a similar inhibitory effect against *C. parapsilosis* to the clinical standards Caspofungin and Fluconazole.

From these results we can see that the NHC*-silver(I) benzoate complexes may be an interesting and effective new class of antimicrobials to be explored and an improvement on previous NHC-silver (I) acetate complexes, such as SBC3, against Gram-negative bacteria, though this is to explored in future work.

Funding

Funding for this research was supplied by the College of Science and School of Chemistry, University College Dublin.

Conflicts of interest

The authors declare no conflicts of interest

Appendix A. Supplementary data

Supplementary data to this article can be found online at https://doi.org/10.1016/j.ica.2018.10.057.

References

[1] A. Gautam, V.C. Ramya, K. Upendranath, S. Srinivasa, Coumarin-tethered (benz) imidazolium salts and their silver(I) N-heterocyclic carbene complexes: synthesis, characterization, crystal structure and antibacterial studies, Appl. Organometal. Chem. 31 (2017) e3770.
[2] Q. Guo, Y. Zhao, X. Dai, T. Zhang, Y. Yu, X. Zhang, C. Li, Functional silver nanocomposites as broad-spectrum antimicrobial and biofilm-disrupting agents, ACS Appl. Mater. Interfaces 9 (2017) 16834–16847.
[3] N.M. Morsi, G.A. Abdelbary, M.A. Ahmed, Silver sulfadiazine based cubosome hydrogels for topical treatment of burns: development and in vitro/in vivo characterization, Eur. J. Pharm. Biopharm. 86 (2014) 178–189.
[4] J.R. Morones-Ramirez, J.A. Winkler, C.S. Spina, J.J. Collins, Silver enhances antibiotic activity against gram-negative bacteria, Sci. Transl. Med. 5 (2013) 190ra81.
[5] S.L. Percival, P.G. Bowler, D. Russel, Bacterial resistance to silver in wound care, J. Hosp. Infect. 60 (2005) 1–7.
[6] P.J. Finley, R. Norton, C. Austin, A. Mitchell, S. Zank, P. Durham, Unprecedented silver resistance in clinically isolated Enterobacteriaceae: major implications for burn and wound management, Antimicrob. Agents Chemother. 59 (2015) 4741–4743.
[7] https://www.cdc.gov/drugresistance/threat-report-2013/index.html; 2013, last accessed: 07/06/2018.
[8] http://www.who.int/drugresistance/documents/surveillancereport/en/; 2014, last accessed: 07/06/2018.
[9] https://ecdc.europa.eu/sites/portal/files/documents/AMR-surveillance-Europe-2016.pdf; 2016, last accessed: 07/06/2018.
[10] R. Laxminarayan, A. Duse, C. Wattal, A.K.M. Zaidi, H.F.L. Wertheim, N. Sumpradit, E. Vlieghe, G.L. Hara, I.M. Gould, H. Goossens, C. Greko, A.D. So, M. Bigdeli, G. Tomson, W. Woodhouse, E. Ombaka, A.Q. Peralta, F.N. Qamar, F. Mir, S. Kariuki, Z.A. Bhutta, A. Coates, R. Bergstrom, G.D. Wright, E.D. Brown, O. Cars, Antibiotic resistance – the need for global solutions, Lancet Infect. Dis. 13 (2013) 1057–1098.
[11] E.D. Brown, E.D. Wright, Antibacterial drug discovery in the resistance era, Nature 529 (2016) 336–343.
[12] A. Melaiye, W.J. Youngs, Silver and its application as an antimicrobial agent, Expert Opin. Ther. Patents 15 (2005) 125–130.
[13] H.J. Klasen, A historical review of the use of silver in the treatment of burns. II. Renewed interest for silver, Burns 26 (2000) 131–138.
[14] Q.L. Feng, J. Wu, G.Q. Chen, F.Z. Cui, T.N. Kim, J.O. Kim, A mechanistic study of the antibacterial effect of silver ions on Escherichia coli and Staphylococcus aureus, J. Biomed. Mater. Res. 52 (2000) 662–668.
[15] W.K. Jung, H.C. Koo, K.W. Kim, S. Shin, S.H. Kim, Y.H. Park, Antibacterial activity and mechanism of action of the silver ion in Staphylococcus aureus and Escherichia coli, Appl. Environ. Microbiol. 74 (2008) 2171–2178.
[16] P. Dibrov, J. Dzioba, K.K. Gosink, C.C. Häse, Chemiosmotic mechanism of antimicrobial activity of Ag(+) in Vibrio cholera, Antimicrob. Agents Chemother. 46 (2002) 2668–2670.
[17] M. Yamanaka, K. Hara, J. Kudo, Bactericidal actions of a silver ion solution on Escherichia coli, studied by energy-filtering transmission electron microscopy and proteomic analysis, Appl. Environ. Microbiol. 71 (2005) 7589–7593.
[18] O. Gordon, T.V. Slenters, P.S. Brunetto, A.E. Villaruz, D.E. Sturdevant, M. Otto, R. Landmann, K.M. Fromm, Silver coordination polymers for prevention of implant infection: thiol interaction, impact on respiratory chain enzymes, and hydroxyl radical induction, Antimicrob. Agents Chemother. 54 (2010) 4208–4218.
[19] B.D. Brooks, A.E. Brooks, Therapeutic strategies to combat antibiotic resistance, Adv. Drug Deliv. Rev. 78 (2014) 14–27.
[20] S. Medici, M. Peana, G. Crisponi, V.M. Nurchi, J.I. Lachowicz, M. Remelli, M.A. Zoroddu, Silver coordination compounds: a new horizon in medicine, Coord. Chem. Rev. 237–238 (2016) 349–359.
[21] S.A. Patil, R. Patil, R.S. Keri, S. Budagumpi, G.R. Balakrishna, M. Tacke, N-heterocyclic carbene metal complexes as bio-organometallic antimicrobial and anticancer drugs, Future Med. Chem. 7 (2015) 1305–1333.
[22] S. Patil, A. Deally, B. Gleeson, H. Müller-Bunz, F. Paradisi, M. Tacke, Novel benzyl-substituted N-heterocyclic carbene–silver acetate complexes: synthesis, cytotoxicity and antibacterial studies, Metallomics 3 (2011) 74–88.
[23] M.A. Sharkey, J.P. O'Gara, S.V. Gordon, F. Hackenberg, C. Healy, F. Paradisi, S. Patil, B. Schaible, M. Tacke, Investigations into the antibacterial activity of the silver-based antibiotic drug candidate SBC3, Antibiotics 1 (2012) 25–28.
[24] N. Browne, F. Hackenberg, W. Streciwilk, M. Tacke, K. Kavanagh, Assessment of in vivo antimicrobial activity of the carbene silver(I) acetate derivative SBC3 using Galleria mellonella larvae, Biometals 27 (2014) 745–752.
[25] C. O'Beirne, H.T. Althani, O. Dada, J. Cassidy, K. Kavanagh, H. Müller-Bunz, Y. Ortin, X. Zhu, M. Tacke, Novel derivatives of the antibiotic NHC–Ag(I) drug candidate SBC3: synthesis, biological evaluation and 109Ag NMR studies, Polyhedron 149 (2018) 95–103.
[26] R. Dorta, L. Shimon, M. Milstein, Rhodium complexes with chiral counterions: achiral catalysts in chiral matrices, J. Organomet. Chem. 689 (2004) 751–758.
[27] H. Jianlin, Y. Shen, C. Li, Y. Li, Y. Pan, Synthesis and characterisation of triphenylphosphine stabilized silver α, β-unsaturated carboxylate: crystal structure of [Ag(O2CCH=C(CH3)2)(PPh3)2], Inorganica Chim. Acta 358 (2005) 4417–4422.
[28] A.J. Arduengo III, R.L. Harlow, M.J. Kline, A stable crystalline carbene, J. Am. Chem. Soc. 113 (1991) 361–363.
[29] W.J. Dolbier Jr., Guide to fluorine NMR for organic chemists, 2nd edition, John Wiley & Sons, New Jersey, United States of America, 2016, p. 17.
[30] F. Hackenberg, G. Lally, H. Müller-Bunz, F. Paradisi, F. Quaglia, W. Streciwilk, M. Tacke, Novel symmetrically p-benzyl-substituted 4,5-diaryl-imidazole N-heterocyclic carbene-silver(I) acetate complexes – synthesis and biological evaluation, J. Organomet. Chem. 717 (2012) 123–134.
[31] S. Patil, A. Deally, F. Hackenberg, L. Kaps, H. Müller-Bunz, R. Schobert, M. Tacke, Novel benzyl- or 4-cyanobenzyl-substituted N-Heterocyclic (bromo)(carbene)silver (I) and (carbene)(chloro)gold(I) complexes: synthesis and preliminary cytotoxicity studies, Helv. Chim. Acta 94 (2011) 1551–1562.
[32] W. Streciwilk, J. Cassidy, F. Hackenberg, H. Müller-Bunz, F. Paradisi, M. Tacke, Synthesis, cytotoxic and antibacterial studies of p-benzyl-substituted NHC-silver(I) acetate compounds derived from 4,5-p-diisopropylphenyl- or 4,5-di-p-chlorophenyl-1H-imidazole, J. Organomet. Chem. 749 (2014) 88–99.
[33] F. Hackenberg, G. Lally, H. Müller-Bunz, F. Paradisi, D. Quaglia, W. Streciwilk, M. Tacke, Synthesis and biological evaluation of N-heterocyclic carbene-silver(I) acetate complexes derived from 4,5-ditolyl-imidazole, Inorg. Chim. Acta 395 (2013) 135–144.
[34] CLSI 2008. Clinical and Laboratory Standards Institute. Reference Method for Broth Dilution Antifungal Susceptibility Testing of Yeasts—Third Edition: Approved Standard M27-A3., USA.
[35] R.C. Clark, J.S. Reid, The analytical calculation of absorption in multifaceted crystals, Acta Crystallogr. A 51 (1995) 887–897.
[36] G.M. Sheldrick, A short history of SHELX, Acta Crystallogr. A 64 (2008) 112–122.